Optimization of Polyethylene/Binder/Polyamide Extrusion Blow-Molded Films. III. Slippability Improvement with Fatty Acid Amides

C. Poisson,[1] V. Hervais,[1] M. F. Lacrampe,[1] P. Krawczak,[1] T. Falher,[2] C. Gondard,[2] V. Ferreiro[3]

[1]*Polymers and Composites Technology and Mechanical Engineering Department, Ecole des Mines de Douai, 941 Rue Charles Bourseul, BP 10838, 59508 Douai Cedex, France*
[2]*Institut Supérieur de Plasturgie d'Alençon, Pôle Universitaire de Montfoulon, 61250 Alençon Damigny, France*
[3]*Unite Mixte de Recherche 8008, Unité de Formation et de Recherche de Physique, Laboratoire de Structure et Propriétés à l'Etat Solide, Université des Sciences et Technologies de Lille, 59655 Villeneuve d'Ascq Cedex, France*

Received 23 July 2007; accepted 20 May 2008
DOI 10.1002/app.30110
Published online 12 October 2009 in Wiley InterScience (www.interscience.wiley.com).

ABSTRACT: The slippability of packaging films has to be controlled to facilitate confectionary operations and guarantee an easy opening for filling. In the case of single-layer polyethylene (PE) films, the addition of slip agents made of fatty acid amides such as erucamide or oleamide usually allows the tailoring of the coefficient of friction (COF) in the film to match industrial targets, which depend on the final application. The coupling of Fourier transform infrared spectroscopy and atomic force microscopy analysis showed that this method has a limited efficiency and may even be detrimental in the case of multilayer PE + ethylene vinyl acetate (EVA)/maleic anhydride grafted polyethylene (PEgMAH) + EVA/polyamide films. The reason is that the migration of the slip additives toward the outermost surface of the PE layer, which leads to a reduction in the COF, are strongly affected by both the existence of the adjacent layers and the presence of EVA in the PE and PEgMAH layers. Nevertheless, a proper knowledge of the effect of this perturbation allows one to reach a slippability level that is required for some confectionary operations and/or for an easy opening for filling without the degradation of the heat sealability. © 2009 Wiley Periodicals, Inc. J Appl Polym Sci 115: 2332–2345, 2010

Key words: additives; atomic force microscopy (AFM); blends; films; FT-IR

INTRODUCTION

The previous studies, reported in parts I and II of this article series, showed that the addition of ethylene vinyl acetate (EVA) in polyethylene (PE) and tie layers of a PE/maleic anhydride grafted polyethylene (PEgMAH)/polyamide (PA) blown film improved the adhesion, heat sealability, and optical properties of the multilayer structure with no negative effect on the mechanical performance.[1,2] Nevertheless, the slippability after manufacturing was significantly reduced [the PE/PE coefficient of friction (COF) increased by 50%]. This can be a major problem for some industrial applications, such as food packaging (easy opening, confectionery, slippability), where the COF has to be maintained in the range 0.2–0.3. In this article, a method is proposed to correct the aforementioned detrimental effect of EVA addition and to improve the slippability.

Correspondence to: M. F. Lacrampe (lacrampe@ensmdouai.fr).

Journal of Applied Polymer Science, Vol. 115, 2332–2345 (2010)

For PE single-layer films, solving this issue may be achieved by the addition of slip agents based on fatty acid amides.[3–14] Their effect is attributed to the incompatibility between the amides and the PE polymer, which induces a migration of these additives toward both external film surfaces.[3–9,14] During film processing, the amides are uniformly distributed in the molten PE. During film cooling and crystallization, they are expelled from the amorphous phase, and then they migrate toward the film surface. Portions of the hydrocarbon chains become embedded in the polymeric matrix and form a molecular bilayer.[4,5] This two-step process leads to a typical evolution of the polymer/polymer COF as a function of time, characterized by a fast decrease (migration and creation of the first layer) followed by a plateau (creation of the second layer; Fig. 1). When this migration process due to the solid state incompatibility between the amides and the polymer is taken into account, the slip agent content can be very low (typically in the range 500–2000 ppm).[5,9,15] Thus, the effect of these additives on the polymer bulk properties is not significant. Only the surface properties are affected. Moreover, the migration

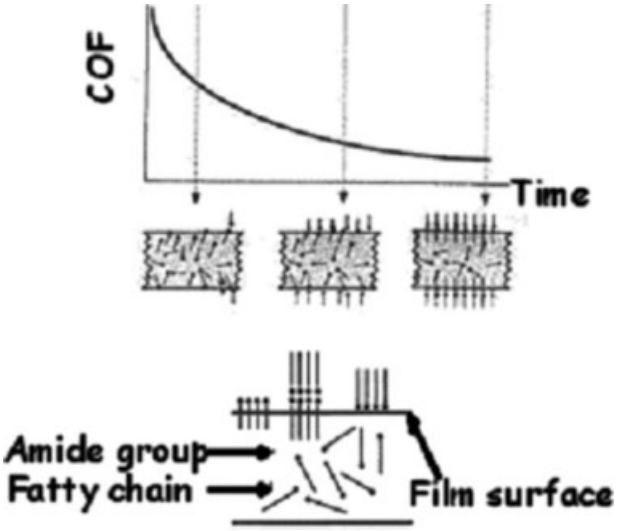

Figure 1 Effect of the slip agent migration on the COF of a polyolefin film.[3,6]

speed essentially depends on the molecular parameters of the slip agent (molecular weight and polydispersity) and on the microstructure (crystallinity degree) of the polymeric matrix, even if it can also be affected by the extrusion processing conditions.[16]

Erucamide (amide derived from monounsaturated C22 erucic acid) and oleamide (derived from monounsaturated C18 oleic acid) are the most commonly used slip agents in the industry (Fig. 2).[3,5,6] Erucamide has a higher molecular weight and migrates slowly. Also, it leads, for equivalent content ratios, to more significant reductions of COF.[4] Therefore, the cheapest oleamide is generally used when the COF has to be reduced directly after film manufacturing (online or out of line after a short postprocessing storage). On the other hand, erucamide is preferred when postprocessing operations are carried out after long storage times in reels or when an online Corona treatment is implemented. Other amides, such as stearamide and behenamide, may also be used, however, with less satisfactory results.[3]

The structural complexity of PE-based multilayer films (with regard to both the stacking sequence and material structure) may modify the dispersion and diffusion mechanisms of the added agents and,

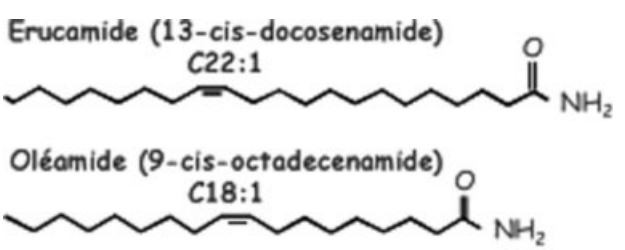

Figure 2 Chemical structures of erucamide and oleamide.[1]

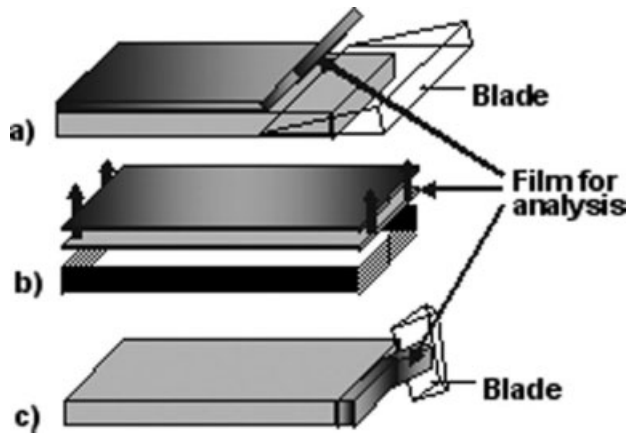

Figure 3 Sample preparation principles for the measurement of the slip agent concentration distribution through the film thickness.

therefore, their efficiency. The effect of such additives on the slippability is, however, rarely reported in the scientific literature.[1,15,17] The published results on this topic tend to show that the efficiency of slip agents may be reduced by the presence of polar adjacent layers, which favor their migration toward the structure inner part.[15,17–20] The migration kinetics then essentially depend on the concentration gradient, the polarity of the different layers, and the temperature.[15,17] Polar amides have a great affinity with polar polymers (e.g., PA and, to a lesser extent, EVA) and, inversely, a very limited affinity with nonpolar polymers (e.g., PE). The perturbation risk of the migration process toward the outermost surface of the PE layer is, therefore, not negligible in a PE + EVA/PEgMAH + EVA/PA multilayer film because of the attraction mechanism toward the structure inner part due to the adjacent layer polarity.[21,22] Identifying this potential perturbation and gaining knowledge about it require the implementation of accurate analysis techniques of the slip additive distribution both on the film surface and in the different layers and of the film surface morphology.

Three methods can be used in practice to determine the distribution of slip agents (or other additives) through the thickness of single or multilayer products.

The first method consists of the use of a microtome to cut very thin material slices parallel to the part surface from the surface toward the core [Fig. 3(a)] and then analysis of each slice by Fourier transform infrared (FTIR) or high-performance liquid chromatography. This method can hardly be applied on thin compliant plastic films.[4,18]

The second method consists of the stacking of many individual single layers, the migration of the additive within this model simulated multilayer,[15,17] and finally, the separation of each layer to analyze it by chromatography after extraction of the additive

[Fig. 3(b)]. This method, however, suffers two major drawbacks. The first one is the practical difficulty in creating a multilayer model, especially for a final product thickness lower than 100 μm. The second is the unknown influence of the different interfaces between layers on the migration process.[15] The multilayer parts produced this way do not fully represent the industrial multilayer extrusion blown films (very low thickness, peculiar thermomechanical history). Nevertheless, this technique has been used to study thick multilayer structures (from 300 up to 800 μm) prepared by the compression molding of individual PE films.[15,17]

In the last alternative method, one uses a microtome that peels slices perpendicularly to the part surface [i.e., cross sections; Fig. 3(c)] from the studied product embedded in wax and then carries out an analysis through-the-product thickness by secondary ion mass spectrometry, surface-enhanced Raman spectroscopy, coherent anti-Stockes Raman spectroscopy, or FTIR microspectroscopy.[23] When used to analyze thin plastic films, these methods may, however, involve some practical issues, such as a quite difficult film positioning with potential deformation induced during the embedding operations or a perturbation of the film microstructure and of the additive migration mechanisms induced by the embedding material (wax). It is, therefore, recommended that one avoid using wax when any organic analysis is planned. A solution may be, in this case, to cool the film sample with liquid nitrogen and/or fix it between two stiff plates to limit its tearing during cutting (especially when very compliant films are considered). Some authors, nevertheless, have chosen to use epoxy wax.[23]

With the broad range of its operating modes and its ability to analyze surfaces under consideration, atomic force microscopy (AFM) is a well adapted tool for characterizing film surface topology and properties.[24–28]

In the tapping mode, the cantilever oscillates vertically at a drive frequency close to its resonance frequency and contacts the sample surface briefly in each oscillation cycle. As the tip approaches the surface, the vibrational characteristics of the cantilever oscillation (e.g., amplitude, resonance frequency, and phase angle) change because of the tip–sample interaction. The surface can be imaged in different ways (height or amplitude images).[26]

In the contact mode [operated in lateral force microscopy (LFM)], the measured lateral force might reflect the tribological properties, which are mainly related to the frictional phenomenon between the sample surface and the cantilever tip. More detailed descriptions of the principles of LFM are found in the pioneering works.[29–31]

Finally, as the slip agents made of fatty acid amides tend to form a lubricating layer at the film's outermost surface, the remaining issue to consider in this article is the influence of the solution proposed to correct the slippability loss induced by previous EVA addition on other postprocessing performance issues, such as heat-sealing ability. Some authors have actually reported that this end-use property may be affected in single-layer PE films.[9,19,32]

In that context, in this study, we aimed to investigate the efficiency of two fatty acid amides (erucamide and oleamide) expected to correct the detrimental effect of EVA addition in multilayer PE/PEgMAH/polyamide 6-66 (PA6-66) packaging films, on one hand, and their ability to improve slippability without a loss in the benefit brought by EVA addition in terms of heat sealing improvement, on the other hand.

The slippability of the multilayer films was assessed through the measurement of the COF. We measured the heat-sealing ability by peeling seals joining the PE sides of two multilayer films. The discussion of the results is based on a coupled FTIR and AFM analysis used to determine a map of the slip agent location through the film thickness and to visualize and quantify its effect on the surface topography and morphology.

EXPERIMENTAL

Materials, manufactured structures, and processing conditions

The study was carried out on three-layer low-density polyethylene (LDPE)/PEgMAH/copolymer PA6-66 blown films with or without 50 wt % EVA (9% vinyl acetate) in the PE and PEgMAH layers. Their main characteristics were reported elsewhere.[1,2] The total film thickness and those of each layer were constant and, respectively, equal to 90 and 50 μm for the PE layer, 10 μm for the tie layer, and 30 μm for the PA6-66 one. The slip agents used were fatty acid amides (erucamide and oleamide) that differed in their number of carbon atoms (Fig. 2). These agents were added with variable contents from 0 to 2500 ppm in the PE layer. The processing conditions were similar to those previously used and reported elsewhere[1,2] and were carefully chosen to prevent interfacial instabilities. It is worth noting that the introduction of the slip agents did not induce perturbation of this interfacial stability.

Slippability testing

The PE/PE dynamic friction coefficient (COF) was measured over a 100-mm distance in the extrusion direction after the film rolls were conditioned at

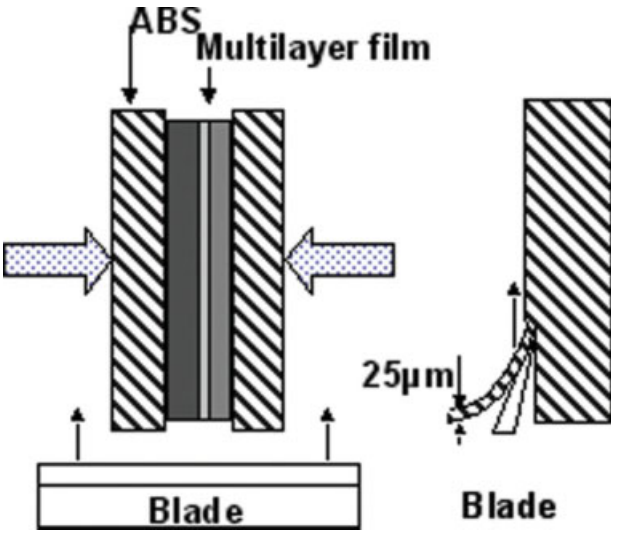

Figure 4 Sample preparation for the IR microscopy analysis.

23°C [50% relative humidity (RH)] for 15 days, according to the NF T 54-112 standard.

Heat-sealing ability testing

The films were sealed with heating jaws (215 × 12 mm^2) onto a Thimonier thermal sealing machine (type SIS-63 CA) (Saint Germain au Mont d'Or, France) with a constant sealing time (0.5 s) and pressure (0.3 MPa) and various sealing temperatures (from 130 to 190°C). The PE/PE seal strength was measured by peeling tests[1,21] on samples (15 × 150 mm) sealed perpendicularly to the extrusion direction.

Microstructure analysis

Attenuated total reflection (ATR) IR spectroscopy

The analysis of the films surface was carried out by FTIR spectroscopy in reflection ATR mode, with a PerkinElmer (Waltham, MA) 1720X instrument. The penetration depth (d_p) during this test depended on the refractive indices of the crystal and the film sample on the considered wavelength and the angle of incidence (α). This method was, therefore, particularly interesting when used to analyze the surface of the films. For a given wavelength characteristic of erucamide (λ = 1650 cm^{-1}, corresponding to the valence vibration of the C=C bond), d_p is 0.4 µm according to the following equation:[33]

$$d_p = \frac{\frac{\lambda}{n_1}}{2\pi\left[\sin^2\alpha - \left(\frac{n_2}{n_1}\right)^2\right]^{1/2}} \quad (1)$$

where n_1 is the refractive index of the crystal (Germanium) and n_2 is the refractive index of the sample, which were equal to 4 and 1.5, respectively, and α was 45°.

For the measurement of the variation of the vinyl acetate, erucamide, and oleamide amounts in reflection ATR mode, the absorption bands centered at 1735, 1633, and 1465 cm^{-1} were, respectively, taken as references for the C=O carbonyl groups of EVA and the slip agents and for the CH_2 groups of the PE chains.

IR microscopy

IR microscopy analyses in specular transmission mode were carried out through the film thickness on a SpectraTech (Oak Ridge, TN) IR-Plan Advantage microscope coupled to a Nicolet 460 ESP Protégé FTIR spectrometer (Thermo Fisher Scientific, France). The samples were cut with a microtome at room temperature (23°C and 50% RH) perpendicularly to the film surface 2000 h after extrusion [Fig. 3(c)]. The microtome device was equipped with a tungsten blade tilted at 8° with respect to the sample. To ensure both homogeneous cutting and absence of contamination, the multilayer film was not embedded in wax but strongly fixed between two acrylonitrile butadiene styrene (ABS) plates. This assembly was placed vertically between the microtome grips (Fig. 4). The cutting thickness is an important parameter that governs the energy required during the FTIR analysis in transmission mode. Experience shows that 25 µm is the optimum thickness, which allows for sufficient energy and a good reproducibility.

The IR spectra of the different layers (PE, PEg-MAH, and PA6-66) were then determined with the so-called double-marking technique at room temperature (23°C and 50% RH) with a meshing aperture of 20 × 80 $µm^2$ with an incremental step of 5 µm

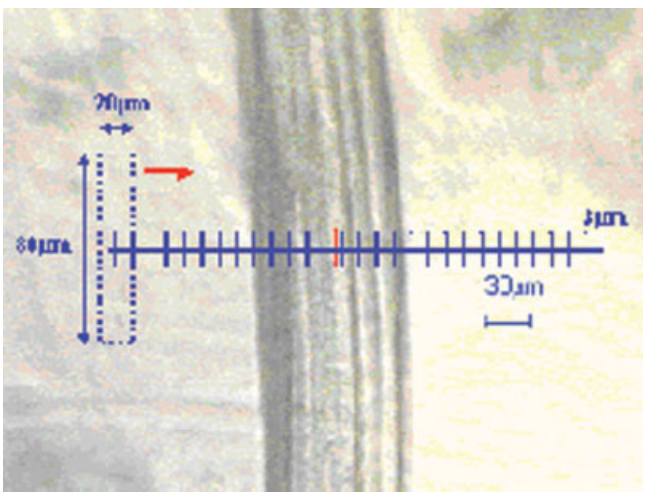

Figure 5 Spatial setup parameters for the IR microscopy analysis. [Color figure can be viewed in the online issue, which is available at www.interscience.wiley.com.]

(Fig. 5). A higher resolution was obtained with 128 scans for each point.

The estimation of the amide-based slip agent concentration gradient was then based on the variation of the C=O valence vibration band (fixed at 1645 cm^{-1}) with respect to the absorbance of the CH_2 strain band (fixed at 1465 cm^{-1} and characteristic of the PE contained in the PE and PEgMAH layers). These two signals were different from the one obtained from vinyl acetate (1740 cm^{-1}; Fig. 6).

The slip agent concentration within the PA6-66 layer could not be measured on the basis of the previous analysis because the characteristic peaks of these amide-based additives and of PA6-66 were superposed. Therefore, they were calculated as the difference between the initially added amount and the sum of the amounts measured on the surface of the PE and PEgMAH layers and within these two layers. The constant weight of the film samples between the film manufacturing period and the IR analysis confirmed the absence of any evaporation of the slip agent as a function of time.

Film surface morphology analysis

The morphology of the films was investigated by AFM. All AFM experiments were carried out in air at room temperature with a NanoScope III multimode microscope from Veeco (Manchester, UK), operating in the tapping mode to visualize the morphology of the sample and in the contact mode (LFM) to measure the difference in mechanical properties (COF).

In the tapping mode, integrated silicon tips with a radius of curvature of about 10 nm were used. Cantilevers (model TSEP) with a nominal spring constant of 40 N/m were used at free oscillation frequencies of about 180 kHz and free oscillation amplitudes in the range 15–30 nm. The images (512 × 512 pixels) were obtained with a piezoelectric scanner (100 × 100 μm^2) at a scanning frequency of 0.5 Hz.

In the contact mode (operated in LFM), the cantilever used in this study was rectangular with a Si3N4 quadrangular pyramid microtip (Olympus Co., Southend-on-sea, UK). The bending constant of the cantilever was 0.13 N/m. To prevent the lateral force caused from cantilever bending, the scanning direction was perpendicular to the long axis of the cantilever. The dependence of the lateral force on the scan rate was investigated in the range 0.1–1 Hz and under a repulsive force of 20 nN at room temperature. The deflection and torsion of the cantilever were measured with a four-segment photodetector with a laser light irradiating the backside of the free end of the cantilever, which were used, respectively, to obtain topographic and lateral force images. The lateral force could be determined from the difference in the histograms of the trace and retrace of LFM images. Topographic contributions to the overall

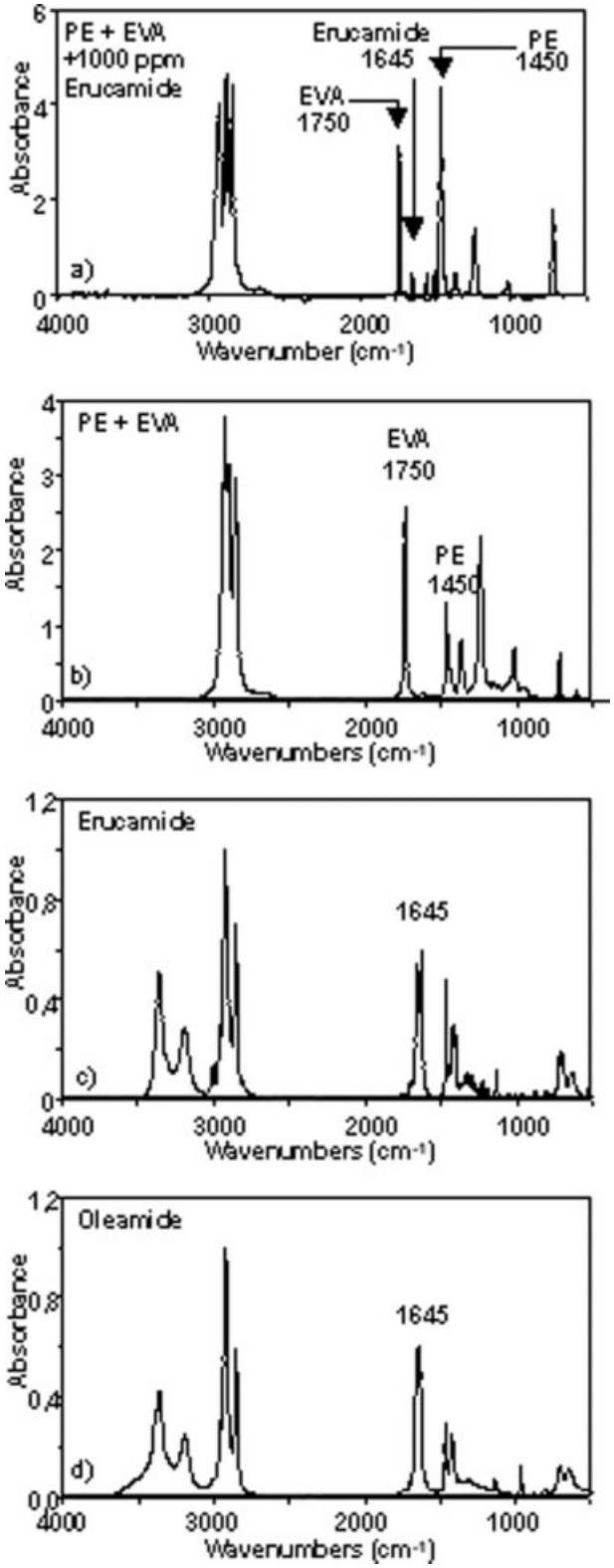

Figure 6 FTIR spectra of (a,b) PE + EVA layers with and without 1000 ppm erucamide, respectively, and (c) neat erucamide and (d) oleamide master batches.

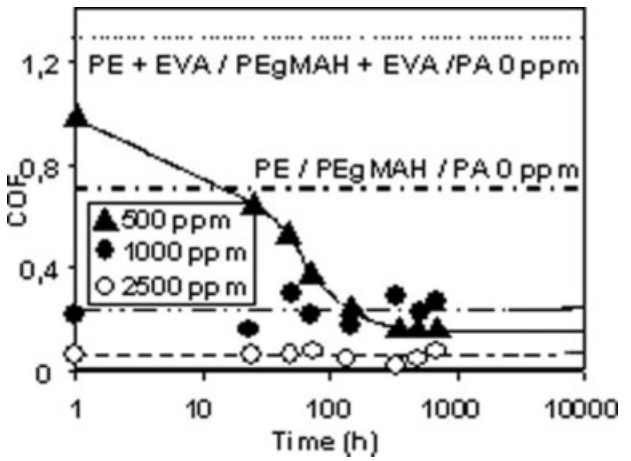

Figure 7 Evolution of the PE/PE COF with time for different erucamide contents in the PE + EVA layer of the PE + EVA/PEgMAH + EVA/PA6-66 films.

lateral force were independent of the scanning direction and, thus, could be removed by the subtraction process. The local COF values are reported as relative values (the value 100 corresponds to the microscopic COF measured on a neat PE film).

RESULTS AND DISCUSSION

Analysis of slip agent global efficiency

Effect of erucamide

Figure 7 shows the effect of the erucamide initial concentration in the PE + EVA layer on the PE side/PE side dynamic COF measured at different times between 0 and 1000 h after extrusion. The ability of this additive to reduce the COF was confirmed. Whatever the slip agent content, the COF was always lower than that of the PE + EVA/PEgMAH/PA film. Nevertheless, at low erucamide contents, the compensation of the negative effect of the EVA introduced into the PE layer was delayed and appeared only 15 h after extrusion. For a 1000-ppm erucamide content, the industrial target ($0.2 < \text{COF} < 0.3$) was instantaneously achieved and was preserved over the entire experimental time range. For a 2500-ppm content, the target was exceeded. The COF instantaneously reached a value of about 0.06, which was then preserved over the investigation time. Finally, for a 500-ppm content, the target was achieved only 100 h after extrusion.

Figure 8 shows the evolution of the seal strength and the associated failure mode for films whose PE + EVA layer contained from 0 to 2500 ppm erucamide and which were sealed at temperatures between 130 and 190°C. The results were normalized (a value of 100 corresponds, for each film, to the maximal seal strength observed between 130 and 190°C). Whatever the erucamide content, the overall features of this curve and the type of failure mode remained unchanged compared to the ones previously noted for the PE/PEgMAH/PA and COF PE + EVA/PEgMAH/PA films.[1,2] Three sealing temperature zones leading to different failure modes were distinguished: separation for sealing temperatures below 140°C, peeling for sealing temperatures between 140 and 160°C, and tearing for sealing temperatures above 160°C.

Also, the peel strength always reached a maximum for a sealing temperature between 160 and 190°C. The failure was always obtained by tearing. This optimal sealing temperature remained almost constant (ca. 160°C) if the erucamide content was lower than 500 ppm and then increased rapidly by approximately 30°C for erucamide contents ranging from 500 to 2500 ppm (Table I). The negative effect of erucamide on the sealability of the films was, therefore, confirmed by the increase in the optimal sealing temperature. Nevertheless, erucamide contents lower or equal to 1000 ppm allowed the preservation of optimal sealing temperatures lower than those of the original PE/PEgMAH/PA multilayer film (without blending with EVA).

Finally, the introduction of erucamide in the PE + EVA layer did not reduce the significant improvement in the sealing temperature range (the temperature range allowing the preservation of at least 94% of the maximum seal strength[21,22]), previously obtained by the addition of EVA to the PE layer[1,2] (Table I). Without EVA, the range of sealability temperatures was very narrow (ca. 10°C). The addition of EVA allowed us to increase this range significantly (up to 35°C) to an extent that was not influenced by the erucamide content. Thus, the addition

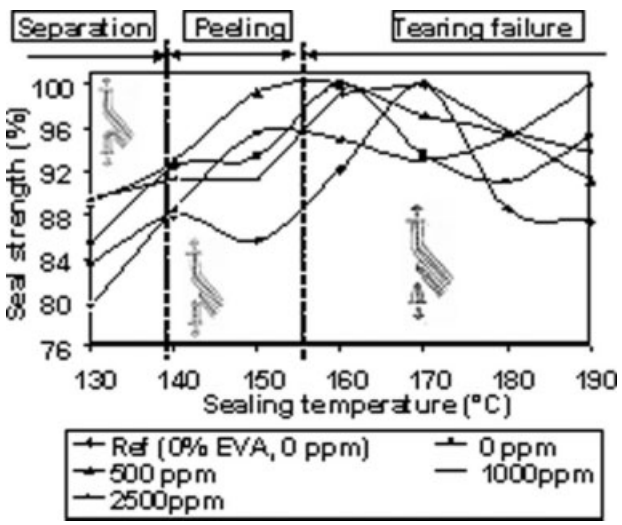

Figure 8 Effect of the sealing temperature on the seal strength for the PE + EVA/PEgMAH + EVA/PA6-66 films with different erucamide contents.

TABLE I
Effects of Additives on the Sealing Ability of PE/PEgMAH/PA6-66 Films With and Without EVA in the PE and PEgMAH Layers

	Nature of the additive	Sealing ability parameter	Additive content (ppm)			
			0	500	1000	2500
PE/PEgMAH/PA6-66		Optimal T (°C)	170			
		ΔT (°C)	10			
PE + EVA/PEgMAH + EVA/PA6-66	Erucamide	Optimal T (°C)	160	160	170	190
		ΔT (°C)	35	40	35	40
	Oleamide	Optimal T (°C)	160	170	160	
		ΔT (°C)	35	22	40	

Optimal T = optimal sealing temperature; ΔT = sealing temperature range.

of erucamide in the PE + EVA layer to get rid of the slippability impairment induced by EVA blending did not diminish the industrial benefit previously achieved in terms of greater flexibility in the control of the sealing process.

Effect of oleamide

The same analysis was carried out for oleamide. For a slip agent content of 1000 ppm, there was a significant reduction in the COF compared to that of the PE + EVA/PEgMAH + EVA/PA film for the entire studied timescale. Moreover, 30 h after extrusion, the COF was even lower than that of the original film composition (PE/PEgMAH/PA; Fig. 9). Nevertheless, this reduction remained low with respect to the industrial target. In contrary, a lower oleamide content led to catastrophic results, characterized by a dramatic increase in the COF. The COF was, in that case, always higher than that of both the original (PE/PEgMAH/PA) and EVA-modified (PE + EVA/PEgMAH + EVA/PA) films. These results were disappointing compared to those reported in the literature for single-layer films, where oleamide was reported as less efficient but more active than erucamide. The addition of EVA in the PE and PEgMAH layers seemed to disturb the oleamide migration mechanism. This could have been related to the short molecular structure of oleamide, which promoted its mobility and affinity with EVA.

Figure 10 shows the relative evolution of the seal strength of films whose PE + EVA layer contained from 0 to 1000 ppm oleamide that were sealed at temperatures between 130 and 190°C (the results are normalized). As for the erucamide, three different sealing temperature zones were distinguished, corresponding to different fracture modes (separation, peeling, and tearing).

However, the presence of oleamide influenced the evolution of the optimal sealing temperature. Thus, the addition of 500 ppm of oleamide ruined the whole benefit in terms of optimal sealing temperature obtained on the optimized structure PE + EVA/PEgMAH + EVA/PA (Table I). For a concentration of 1000 ppm (which led to a significant improvement of the slippability even if not sufficient), the positive effect of the incorporation of EVA

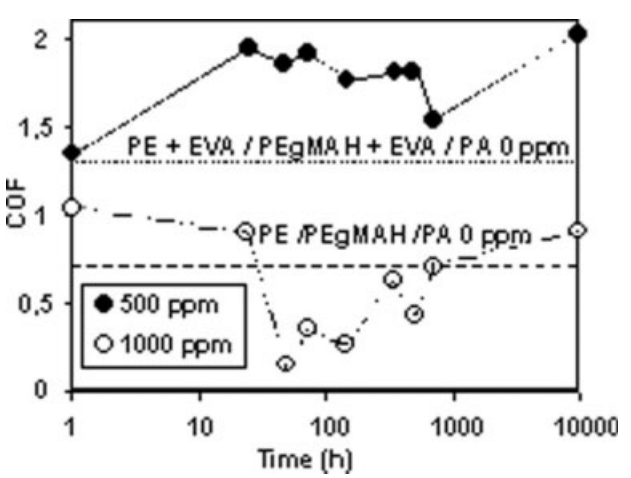

Figure 9 Evolution of the PE/PE COF with time for different oleamide contents in the PE + EVA layer of the PE + EVA/PEgMAH + EVA/PA6-66 films.

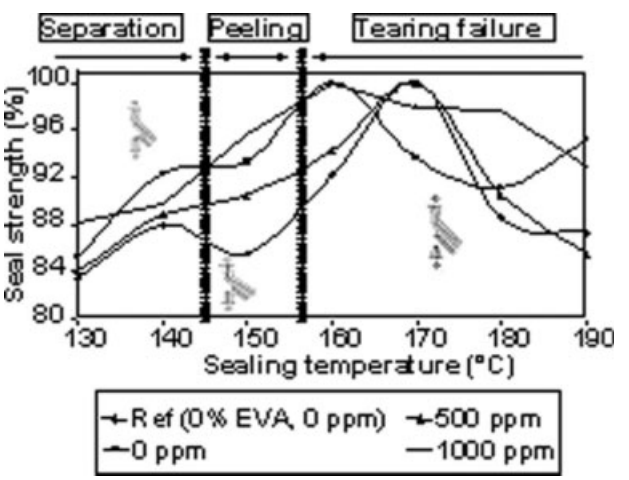

Figure 10 Effect of the sealing temperature on the seal strength for the PE + EVA/PEgMAH + EVA/PA6-66 films with different oleamide contents.

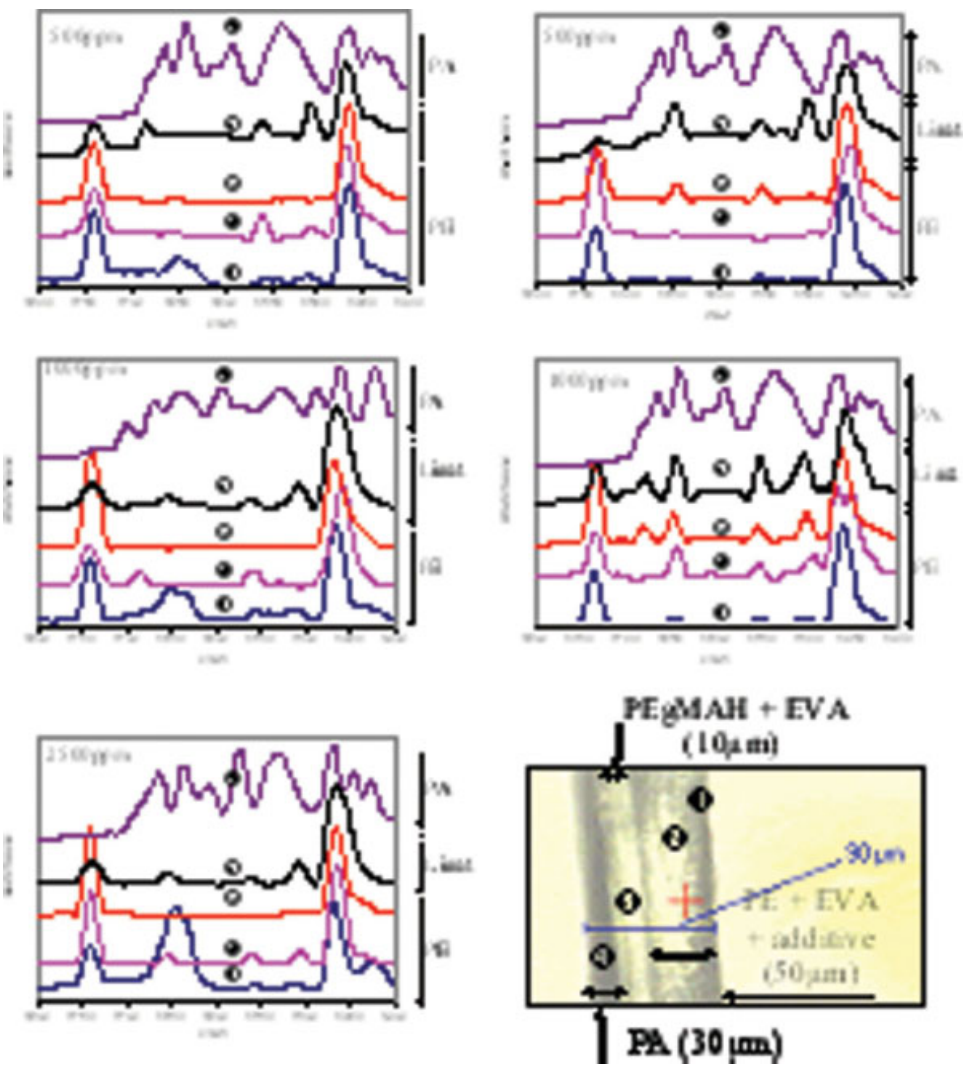

Figure 11 FTIR spectra of the PE/PEgMAH/PA6-66 films with a slip agent (1000 ppm) in PE + EVA: (1) PE surface in the ATR mode (>0.4 µm) and (2) surface of the PE layer (>3 µm), (3) middle of the PE layer, (4) tie layer, and (5) PA layer in IR microscopy. [Color figure can be viewed in the online issue, which is available at www.interscience.wiley.com.]

on the optimal sealing temperature was totally recovered. Moreover, the addition of oleamide in the PE + EVA layer notably affected the range of sealing temperature (Table I). This temperature showed a minimum for a concentration of 500 ppm. However, whatever the oleamide content, the heat-sealing ability impairment was not important enough to fully ruin the benefit brought by the addition of EVA in the PE layer to improve sealability.[1,2]

Through-the-thickness structure analysis by FTIR

Figures 11 shows the FTIR spectra obtained 1000 h after extrusion on the PE + EVA/PEgMAH + EVA/PA films containing 500, 1000, and 2500 ppm of erucamide [Fig. 11(a)] or oleamide [Fig. 11(b)] in the PE + EVA layer.

In the case of erucamide, whatever its initial concentration, the slip additive (peak at 1633 cm^{-1}) was mainly present in a very thin area of the outermost surface (over about 0.4 µm) of the PE + EVA layer. Then, the concentration decreased for a 3-µm depth and reached a minimum within this PE + EVA layer [Fig. 11(a)]. Erucamide was also detected in the PEgMAH tie layer. Because of the superposition of the FTIR peaks of erucamide and PA, the presence or absence of this slip additive in the PA layer could not be determined this way. Moreover, there was a relationship between the slip agent content added to the PE + EVA layer, the PE side/PE side COF, and the concentration of erucamide on the film surface (Fig. 12). The reduction in the COF was directly related to the amount of erucamide on the film surface. It logically increased with the initial concentration of additive and/or the time after extrusion. Finally, the parasitic and negative effects of the EVA in the PE layer on the erucamide efficiency was clearly highlighted (Fig. 12). For a given surface

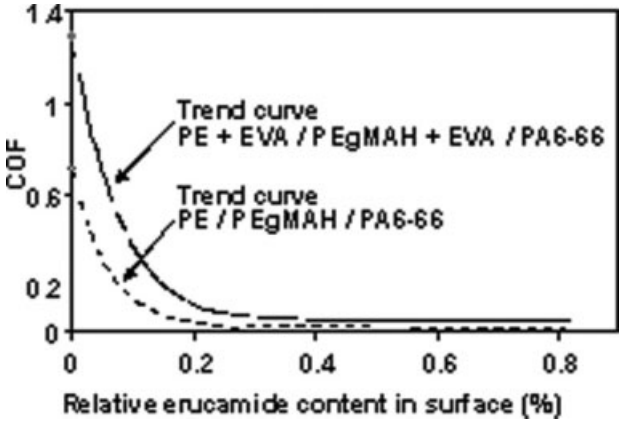

Figure 12 Evolution of the PE/PE COF with the erucamide content at the film surface (measured by FTIR in the ATR mode, initial bulk content = 1000 ppm).

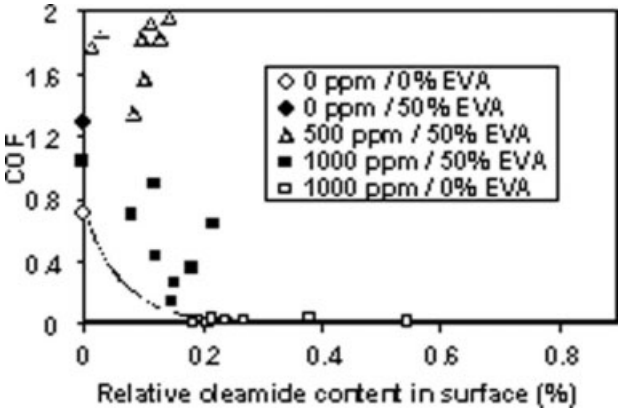

Figure 14 Evolution of the PE/PE COF with the oleamide content at the film surface (measured by FTIR in the ATR mode).

concentration of erucamide, the COF of the PE + EVA/PEgMAH + EVA/PA film was always higher than the one of the PE/PEgMAH/PA structure.

In the case of oleamide, whatever its initial concentration, a quite low amount of slip additive was present in a very thin area next to the surface (over about 0.4 μm) of the PE + EVA layer. Then, the concentration decreased for a 3-μm depth and reached a minimum within this PE + EVA layer. This minimum was closer to the surface than for erucamide. Finally, the oleamide concentration increased again in the tie layer (Fig. 13). Moreover, contrary to erucamide, there was no correlation between the global concentration of added oleamide, the COF, and the surface concentration of slip additive (Fig. 14). However, as for erucamide, the parasitic effect of the addition of EVA into the PE layer on the efficiency of oleamide was clearly identified.

This efficiency difference of both slip agents in the films containing EVA or not could have different explanations.

First, the slip agent that migrated toward the surface may not have homogeneously covered the entire surface. As a result, lubricant-noncovered areas were still present on the surface. These areas were made of PE and EVA in similar proportions. As EVA is intrinsically less slipping than PE and affects the crystalline morphology of PE, this resulted in a reduced slippability of the PE + EVA blend. However, this hypothesis was not sufficient to explain the discrepancies observed in the two types of films. For a given surface concentration of slip additive, the COF ratio between the two film formulations was not constant, whereas the PE/EVA ratio was constant (Fig. 15).

Therefore, the higher affinity of the slip agents with EVA may also have been an effect that was combined with the previous one. Thus, for a similar surface concentration of additive, the slip agent would not have been homogeneously distributed between the two components of the PE + EVA layer

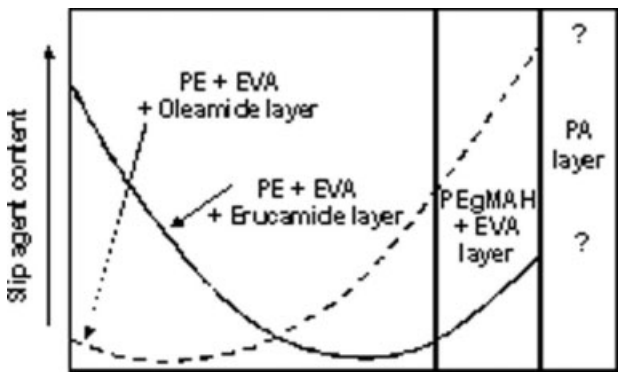

Figure 13 Schematic distribution of the slip agents through the PE + EVA/PEgMAH + EVA/PA6-66 film thickness.

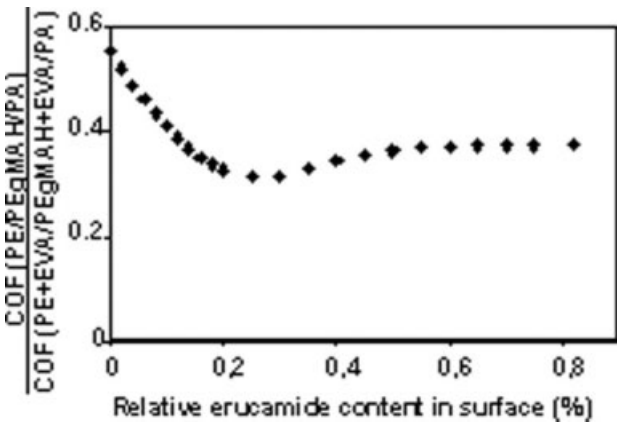

Figure 15 Evolution of the PE/PEgMAH/PA6-66 COF/PE + EVA/PEgMAH + EVA/PA6-66 COF ratio with the erucamide content on the film surface.

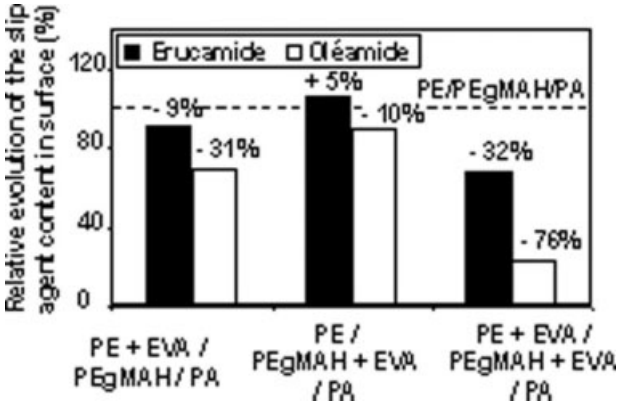

Figure 16 Effect of EVA and PEgMAH on the slip agent content on the film surface (initial slip agent bulk content = 1000 ppm).

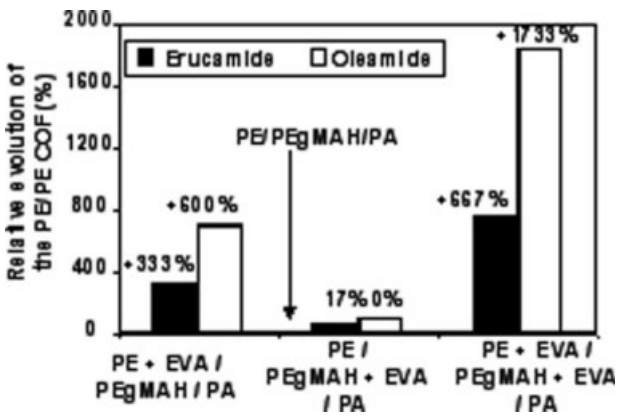

Figure 17 Effect of EVA and PEgMAH on the PE/PE COF (initial slip agent bulk content = 1000 ppm).

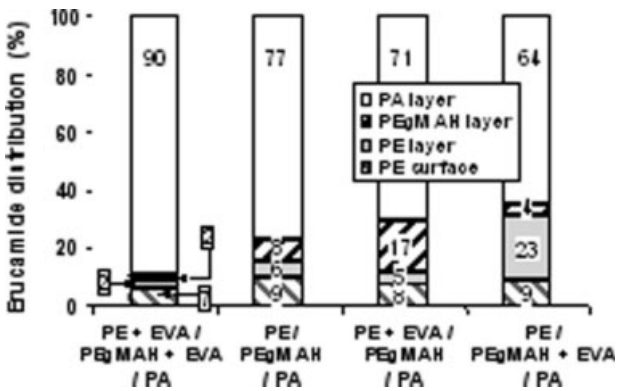

Figure 18 Erucamide distribution in different layers for the PE and PEgMAH layers containing or not containing EVA (initial erucamide content = 1000 ppm).

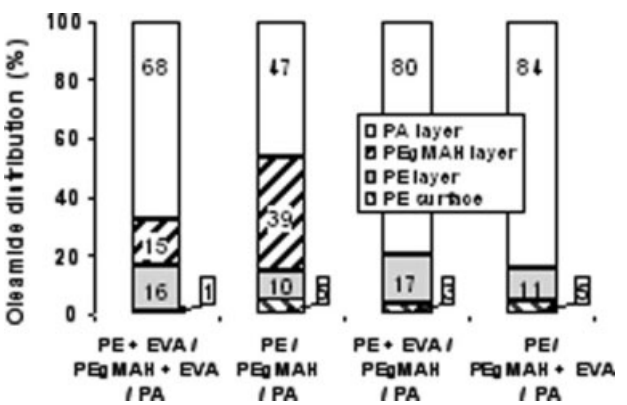

Figure 19 Oleamide contents in different layers for the PE and PEgMAH layers containing or not containing EVA (initial oleamide content = 1000 ppm).

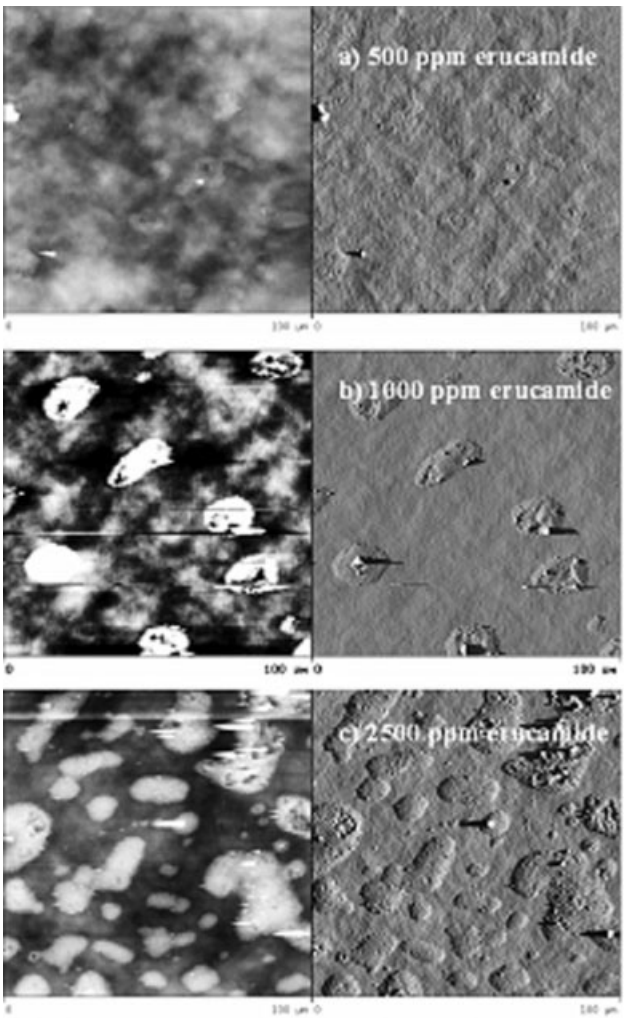

Figure 20 AFM surface analysis of the PE + EVA face of a multilayer film [(50% PE + 50% EVA + erucamide)/(PEgMAH + 50% EVA)/PA] as a function of the initial erucamide content.

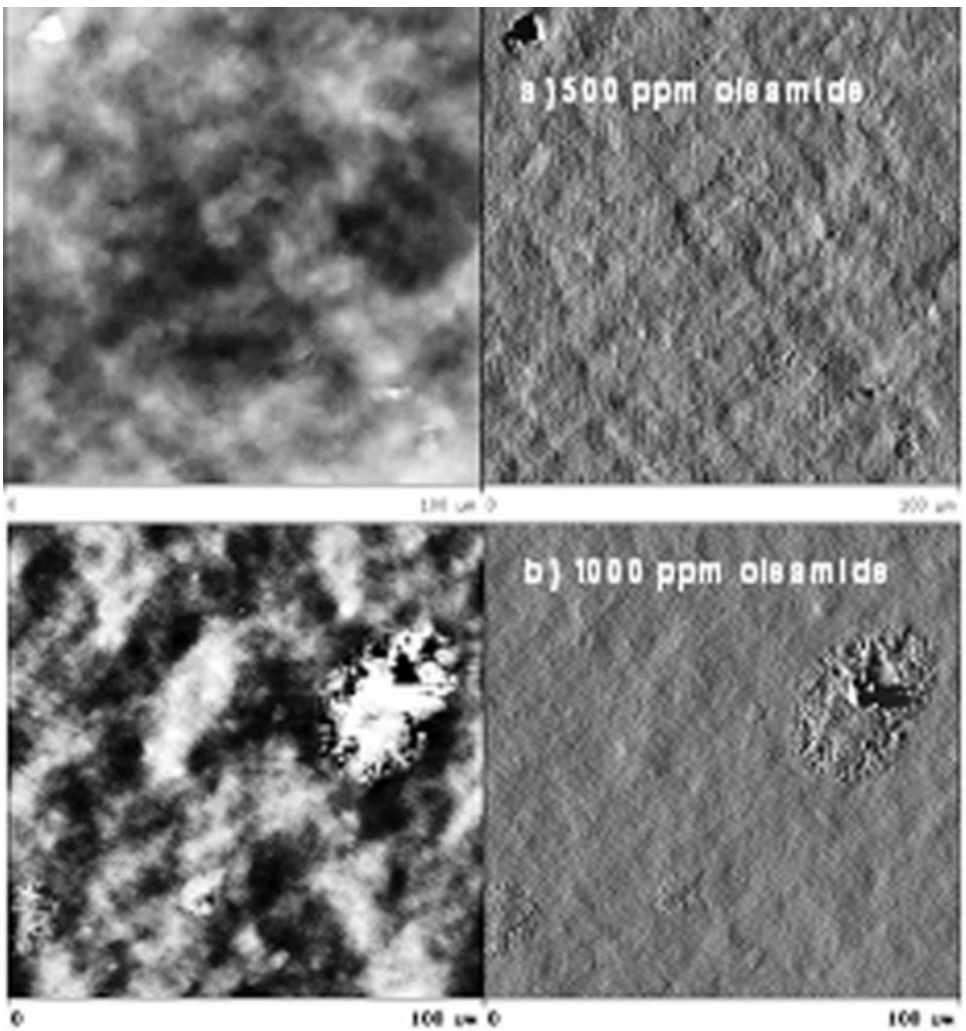

Figure 21 AFM surface analysis of the PE + EVA face of a multilayer film [(50% PE + 50% EVA + oleamide)/(PEgMAH + 50% EVA)/PA] as a function of the initial oleamide content.

but would be mainly concentrated in the EVA-rich areas. Then, the lubricating effect on the PE would have then been reduced. The validity of this assumption was later verified by AFM analysis.

Furthermore, the presence of adjacent polar layers influenced the migration process of erucamide through the film. For an initial slip agent concentration of 1000 ppm and at an equilibrium surface concentration (1000 h), the addition of EVA in the PE and/or PEgMAH layers resulted in a significant reduction of the slip agent migration toward the film surface (Fig. 16) and in a notable increase of the COF (Fig. 17) with a higher amplitude when oleamide was used. The validity of this last hypothesis could be checked by the integration of the curves (on the basis of FTIR mapping) to give the evolution of the slip agent concentrations in the PE and PEgMAH layers containing EVA or not and by the estimation of the slip agent concentration in the PA layer by the difference between the total slip agent amount initially added and the amounts measured in the two other layers (FTIR analysis was not possible due to the superposition of the characteristic peaks of the amide-based slip agents and PA).

Figures 18 and 19 show the distribution of erucamide (Fig. 18) and oleamide (Fig. 19) on the outermost surface and within the PE, PEgMAH, and PA6-66 layers of the films with or without EVA in the PE and/or PEgMAH layers.

In the case of erucamide

- When EVA was added to the PE layer, the surface concentration of slip agent was reduced (Fig. 16) because of the migration effect of erucamide toward the PEgMAH tie layer (+225%; Fig. 18).
- When EVA was added to the PEgMAH layer, the total amount of slip agent in the PE layer was 3.8 times higher. However, the surface concentration of erucamide remained the same (Fig. 16 and 18), and consequently, the COF did not change.

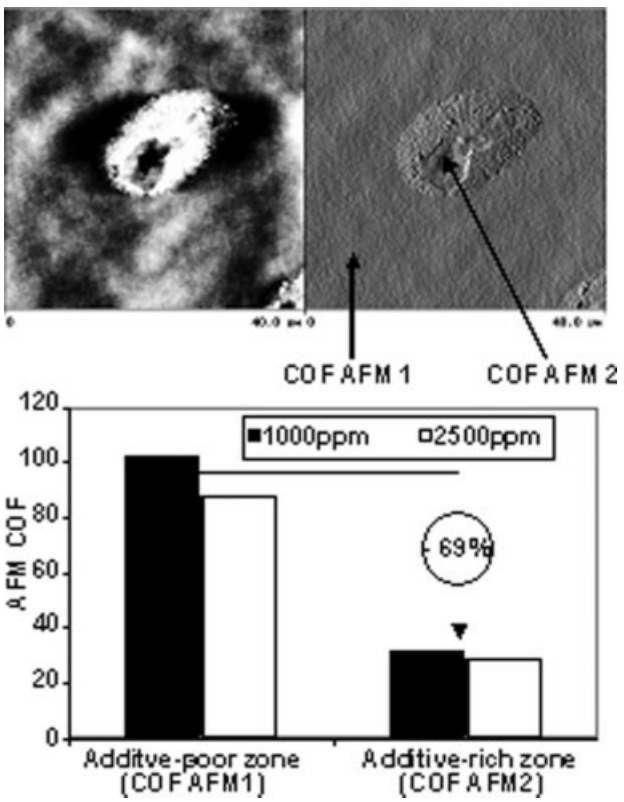

Figure 22 Variation of the local COF measured by AFM in different zones of a PE + EVA/PEgMAH + EVA/PA 6-66 film containing erucamide.

- When EVA was added to both the PE and PEgMAH layers, the surface concentration of slip agent was significantly reduced (Fig. 16 and 18) because a strong migration of erucamide was observed within the PA6-66 layer (+17%).

As a result, erucamide seemed to concentrate in the EVA-poor zones and tended to migrate significantly toward and within the PA layer (with the content reaching between 64 and 90% in this layer).

In the case of oleamide, the slip agent migration toward the PA6-66 layer also explained the variations in the surface concentration of oleamide when EVA was added to either the PE or PEgMAH layer.

Surface morphology analysis by AFM

The film surface observation by AFM in tapping mode showed that, whatever the added slip agent, the additive did not homogeneously migrate toward the surface. It formed mushroomlike shapes, whose sizes and distribution depended on its initial concentration (Figs. 20 and 21). The measurement of the local COF by AFM pointed out that the mushroomlike shapes corresponded to a high concentration of slip agent. The COF measured was about 70% lower than that of the remaining surface, whatever the type and the initial concentration of the slip additive (Fig. 22).

Figure 23 shows the global and local COF measured on a macroscopic scale on a tensile machine or at a microscopic scale by AFM (AFM1 is the additive-poor zone, and AFM2 is the additive-rich champignon, as defined in Fig. 22), respectively, for the various films containing erucamide and/or EVA or not.

Whatever the erucamide initial concentration, the local COF of the additive-poor zones was the same, close to that of a neat PE film. The local COF of the additive-rich regions was constant as well; however, it was much lower than the previous one. The reduction of the global COF induced by the addition of erucamide was, therefore, clearly linked to the creation of additive-rich areas on the film surface. However, the decrease of the global COF between 500 and 2500 ppm erucamide may only have been related to an increase of the surface density of the mushroomlike shapes of constant local COF. This increased the contact surface between the sole and the film and was confirmed by the AFM analysis (Fig. 24). The surface density of the additive-rich regions actually rose from 17 to 30% (+69%) between 1000 and 2500 ppm of added slip agent, whereas the global COF dropped in similar proportions (70%).

Similar differences (ca. 60%) between the local COFs of the additive-rich and additive-poor regions were observed when oleamide was used as the slip agent (Fig. 25). It was, nevertheless, not possible to explain the difference noticed between the two additives on the basis of these data only. Also, the size and surface distribution of the mushroomlike shapes were fully different at the same given initial concentration for erucamide and oleamide. For example, the nodule surface density was estimated at 12% for

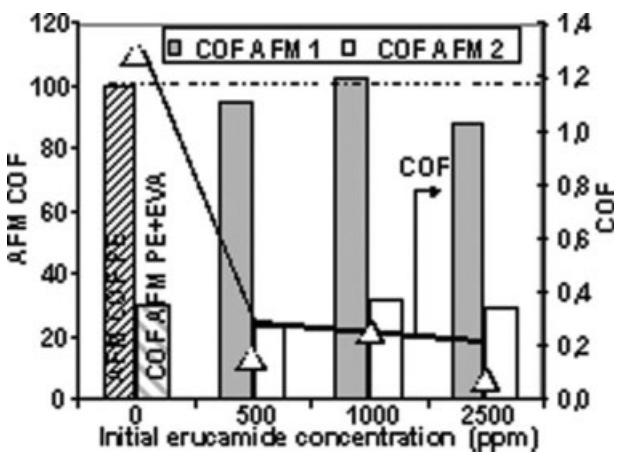

Figure 23 Variation of the global and local COF as a function of the erucamide concentration in the PE and PE + EVA layers.

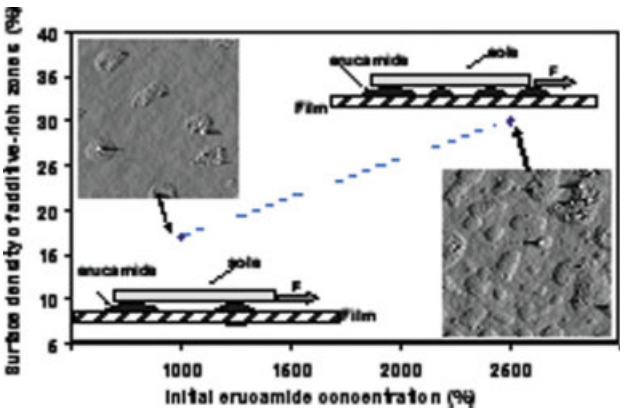

Figure 24 Evolution of the surface density of additive-rich zones (mushroomlike shapes) as a function of the slip agent concentration in the PE layer. [Color figure can be viewed in the online issue, which is available at www.interscience.wiley.com.]

oleamide and 17% for erucamide (a 30% difference). Moreover, the additive-rich nodules almost all had the same size for erucamide, whereas those of the oleamide mushroomlike shapes varied much more (the existence of a lot of small nodules), which resulted in a reduced sole/film effective contact surface (Fig. 26).

Figures 23 and 25 show that, whatever the slip agent, the local COF of the additive-rich regions was close to that of the PE + EVA blend, whereas that of the additive-poor regions was close to that of neat PE. This tended to prove that the mushroomlike shapes were located on the EVA-rich regions. The assumption of the preferential migration of these slip additives toward areas of higher polarity (e.g., the vinyl acetate at the surface of the PE + EVA layer and the adjacent layers) was thus confirmed

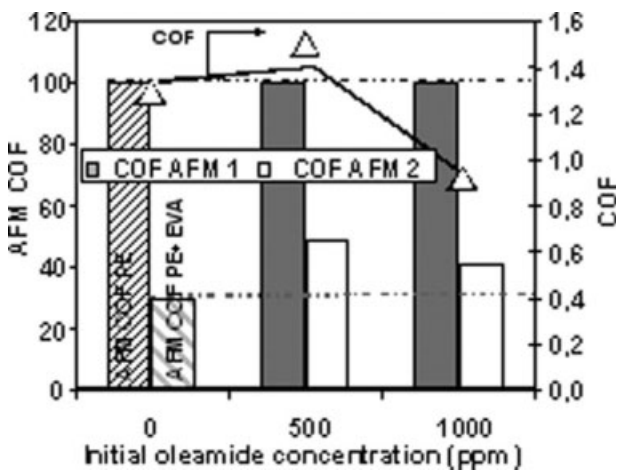

Figure 25 Variation of the global and local COF as a function of the oleamide concentration in the PE and PE + EVA layers.

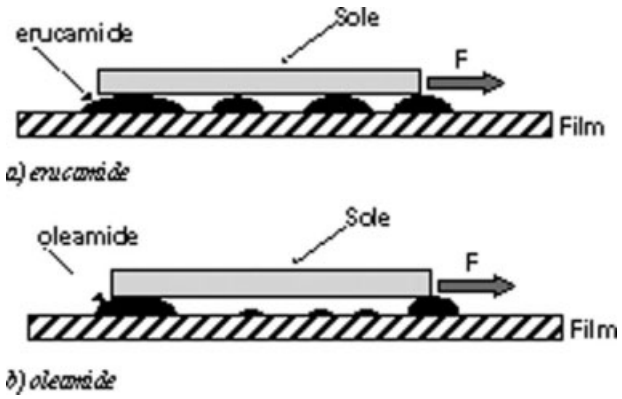

Figure 26 Scheme of the macroscopic COF test carried out on films containing different slip agents.

and explained their reduced efficiency compared to the case of a multilayer film without EVA.

CONCLUSIONS

The impairment of the slippability of multilayer PE/PEgMAH/PA6-66 blown films containing EVA in the PE and tie layer for the purpose of heat-sealing ability and interlayer adhesion improvement was corrected by the addition of low amounts of unsaturated fatty acid amide additives in the PE + EVA layer. This result could be achieved without a loss in the benefit brought by EVA in terms of heat-sealing ability, as long as the slip agent type and concentration were optimized.

Two different fatty acid amide-based slip additives (erucamide and oleamide) were tested Erucamide is recommended because the use of oleamide may result in undesirable effects (an increase of the COF and/or loss of the sealability improvement brought by EVA). Whatever the type of fatty acid amide used, the decrease in the COF was, however, lower than those reported in the literature for single-layer PE films. This was attributed to the existence of a perturbation of their migration mechanisms toward the outermost film surface after film manufacturing.

The FTIR spectra determined on film cross sections actually highlighted the presence of a significant amount of slip agent in the film core (in particular, in the polar PEgMAH layer) and in the PA6-66 layer. The additives were, therefore, less concentrated on the PE + EVA surface and were, consequently, less efficient for reducing the COF. This lack of slip agent at the film surface was much more important for oleamide than for erucamide. Furthermore, the presence of EVA in the PE layer still amplified the slip agent migration toward the PEgMAH layer. This phenomenon may have been partly limited for erucamide when the PEgMAH layer also contained EVA.

The AFM analysis of the outermost surface of the multiplayer films showed that the additive, which migrated toward the surface, was heterogeneously distributed in the form of mushroomlike shapes mainly located in EVA-rich regions. Compared to EVA-free films, the reduced efficiency of the slip agents may then be attributed to the decrease of the effective slipping surface. The efficiency difference noticed between erucamide and oleamide additives may be explained by a significant difference in the size and surface density of the additive-rich nodules.

The authors thank J. M. Coillot for his contribution to the film manufacturing.

References

1. Poisson, C.; Hervais, V.; Lacrampe, M. F.; Krawczak, P. J Appl Polym Sci 2006, 99, 974.
2. Poisson, C.; Hervais, V.; Lacrampe, M. F.; Krawczak, P. J Appl Polym Sci 2006, 101, 118.
3. Maltby, A. J. In Proceedings of the 2002 PLACE Conference, Boston, MA, Sept 2002; TAPPI: Atlanta, GA, 2002; Session 17, Paper 65, p 9.
4. Maltby, A. J.; Marquis, R. E. In Proceedings of the 1996 Polymers, Laminations and Coatings Conference, Boston, MA; TAPPI: Atlanta, Georgia, Sept 1996; Vol. 1, p 25.
5. Coupland, K.; Maltby, A. J.; Parker, D. A. Presented at Addcon Asia '97, Singapore, Oct 1997; Paper 15; RAPRA: Shawbury, Shopshire, UK.
6. Glover, J. H. In Proceedings of the 1987 Polymers, Laminations, and Coatings Conference, Sept 1987, San Francisco, CA; TAPPI: Atlanta, Georgia, Vol. 1, p 231.
7. Maltby, A. J.; Buxton, P. Polym Polym Compos 1999, 7, 537.
8. Walp, L.; Breuer, T. In Proceedings of the 2000 TAPPI Polymers, Laminations and Coatings Conference, Chicago, IL; TAPPI: Atlanta, Georgia, Aug 2000; Vol. 2, p 927.
9. Rinker, J. W. Pap Film Foil Converter 1980, 54, 45.
10. Chen, B. L. In Proceedings of the 1997 TAPPI Polymers, Laminations and Coatings Conference, Toronto, Canada; TAPPI: Atlanta, Georgia, Aug 1997; Vol. 2, p 427.
11. Maltby, A. J.; Read, M. In Proceedings of the 1999 Polymers, Laminations and Coatings Conference, Atlanta, GA; TAPPI: Atlanta, Georgia, Aug 1999; Vol. 2, p 1079.
12. Maltby, A. J. In Proceedings of the 1999 Polymers, Laminations and Coatings Conference, Atlanta, GA; TAPPI: Atlanta, Georgia, Aug 1999; Vol. 1, p 349.
13. Schumann, B. H.; Wooster, J. J. In Proceedings of ANTEC '99, New York, NY; Society of Plastics Engineers (SPE): Brookfield, Connecticut, May 1999; Vol. 1, p 46.
14. Muire, L. B.; Hirt, D. E. In Proceedings of ANTEC 2000, Orlando, FL; Society of Plastics Engineers (SPE): Brookfield, Connecticul, May 2000; Paper 567.
15. Bryant, K. A. A. In Proceedings of the 1998 Polymers, Laminations and Coatings Conference, San Francisco, CA; TAPPI: Atlanta, Georgia, Sept 1998; Vol. 1, p 969.
16. Wooster, J. J.; Simmons, B. E. J Plast Film Sheeting 1996, 12, 50.
17. Hirt, D. E.; Sankhe, S. Y. Appl Spectrosc 2002, 56, 205.
18. Joshi, N. B.; Hirt, D. E. Appl Spectrosc 1999, 53, 11.
19. Sankhe, S. Y.; Hirt, D. E. Appl Spectrosc 2002, 56, 205.
20. Shankhe, S. Y.; Javorkar, A. V.; Hirt, D. E. J Plast Film Sheeting 2003, 19, 16.
21. Poisson, C. Ph.D. Thesis, Université de Lille 1, 2005.
22. Poisson, C.; Hervais, V.; Lacrampe, M. F.; Krawczak, P. In Proceedings of the 21st Annual Meeting of the Polymer Processing Society, Leipzig, Germany; Martin Luther University Halle-Wiitenberg, Hall, Germany, June 2005; Paper 1.18.
23. Jouan, X.; Gardette, J. L. Polym Commun 1987, 28, 239.
24. Magnov, S. N.; Elings, V.; Papkov, V. S. Polymer 1996, 38, 297.
25. Magonov, S. N.; Elings, V.; Whangbo, M. H. Surf Sci 1997, 375, L385.
26. Magonov, S. N.; Cleveland, J.; Elings, V.; Denley, D.; Whangbo, M. H. Surf Sci 1997, 389, 201.
27. Fasolka, M. J.; Mayes, A. M.; Magonov, S. N. Ultramicroscopy 2001, 90, 21.
28. Persyn, O.; Miri, V.; Lefevbre, J. M.; Ferreiro, V.; Brink, T.; Stroeks, A. J Polym Sci Part B: Polym Phys 2005, 44, 1690.
29. Gibson, C. T.; Watson, G. S.; Myhra, S. Wear 1997, 203, 71.
30. Carpick, R. W.; Ogletree, F.; Salmeron, M. Appl Phys Lett 1997, 70, 1548.
31. Ling, J. S. G.; Legget, G. J.; Murray, A. J. Polymer 1998, 39, 5913.
32. Foldes, E.; Szigeti-Erdej, A. In Proceedings of ANTEC '97, Toronto, Canada, April-May 1997; Society of Plastics Engineers (SPE): Brookfield, Connecticut, Vol. III, p 3024.
33. Chenery, D. H.; Sheppard, N. Appl Spectrosc 1978, 32, 798.